

DOI: 10.1002/cctc.201300783

Pressure-Dependent Effect of Hydrogen Adsorption on Structural and Electronic Properties of Pt/ γ -Al₂O₃ Nanoparticles

Hemma Mistry,^[a] Farzad Behafarid,^[a] Simon R. Bare,^[b] and B. Roldan Cuenya^{*[a, c]}

Understanding the interaction of hydrogen with subnanometer platinum nanoparticles (NPs) under industrially relevant conditions is of great importance to heterogeneous catalysis. In this work, we investigate the pressure-dependent changes in hydrogen coverage on size- and shape-selected Pt/ γ -Al₂O₃ NPs by in situ X-ray absorption near-edge structure (XANES) analysis. Difference XANES calculations revealed an increase in the H/Pt ratio from 1.9 to 2.5 upon increasing the hydrogen pressure from 1 to 21 bar at room temperature (1 bar = 100 kPa). In

addition, extended X-ray absorption fine structure measurements of the local geometrical structure showed changes in Pt–Pt bond length and coordination number, revealing a morphological transformation in the NPs from a 2D to a 3D shape under increasing H₂ pressure at room temperature. Such shape evolution leads to a decrease in the NP–support contact area and is thus expected to affect the NP stability against coarsening.

Introduction

The interaction of hydrogen with supported noble-metal nanoparticles (NPs) is of great interest in heterogeneous catalysis, especially for applications such as hydrogenation reactions,^[1] electrocatalysis,^[2] and hydrogen storage.^[3] Recent research has shown many of these catalytic processes to be dependent on catalyst particle size and shape.^[4] Smaller, subnanometer-sized particles are often more active because of the increased number of edge and corner sites. For some chemical processes, these properties might correspond to the increased ability of such small NPs to adsorb hydrogen,^[5] which has received much attention in recent literature, particularly for the Pt/Al₂O₃ system.^[6] On Pt(111) single crystals, hydrogen coverage has been measured to saturate at a 1:1 ratio of H/Pt, a fact commonly used to calibrate metallic surface area measurements.^[7] However, H₂ chemisorption isotherm measurements have indicated that nanometer-sized particles can adsorb between 1.1 to 1.5 H atoms per Pt.^[8] Theoretical work has predicted even higher hydrogen coverages for subnanometer Pt particles,^[9] such as Pt₁₃ NPs which can stabilize 3.3 H/Pt as a result of par-

ticle shape reconstruction.^[6c] Using size- and shape-selected Pt/ γ -Al₂O₃ NPs, Behafarid et al.^[6a] observed experimentally that small NPs with a large number of low-coordinated surface atoms (corner and edge sites) can adsorb significantly more H/Pt at atmospheric pressure than larger, more bulk-like NPs.


Understanding the adsorption of hydrogen on NP surfaces has been challenging because of the complex interplay between particle structure and electronic properties, adsorbate interactions, and support effects.^[6a, 10] Furthermore, under realistic reaction pressures and temperatures, NPs can have a dynamic structure which allows them to transition between several stable structural isomers,^[6c, 11] which further complicates their characterization. Several recent studies have measured morphological changes in Pt NPs under hydrogen environments.^[8c, 12] Particularly interesting are recent theoretical investigations by Mager-Maury et al.,^[6c] who calculated structural changes in subnanometer Pt/ γ -Al₂O₃ NPs as a function of temperature and pressure. Their theoretical work predicts that an increase in the H coverage should result in Pt₁₃ NPs evolving from a biplanar to a cuboctahedral morphology as a result of weakened metal–support interactions and surface Pt hydride formation.^[6c]

In situ X-ray absorption near-edge structure (XANES) spectroscopy at the Pt L₃-edge has proved to be an excellent tool for the study of hydrogen adsorption on Pt NPs through observing changes in the d electron density of states of the particles under different adsorbate environments.^[6a, 8c, 10b, c, 12a, 13] In this experimental work we investigate the pressure-dependent changes in hydrogen coverage on size- and shape-selected Pt/ γ -Al₂O₃ NPs as well as on their structure by using in situ XANES and extended X-ray absorption fine structure (EXAFS) spectroscopy measurements. Difference XANES (Δ XANES) plots were used to quantify the H/Pt ratio as a function of H₂ pres-

[a] H. Mistry, Dr. F. Behafarid, Prof. B. Roldan Cuenya
Department of Physics
University of Central Florida
Orlando, FL 32816 (USA)
E-mail: roldan@ucf.edu

[b] Dr. S. R. Bare
UOP LLC, a Honeywell Company
Des Plaines, IL 60017 (USA)

[c] Prof. B. Roldan Cuenya
Department of Physics
Ruhr University Bochum
Bochum (Germany)
E-mail: Beatriz.Roldan@rub.de

 Supporting information for this article is available on the WWW under <http://dx.doi.org/10.1002/cctc.201300783>.

sure. In addition, EXAFS measurements showed changes in Pt–Pt bond length and coordination number, revealing morphology changes in the Pt NPs at room temperature under increasing H₂ pressure.

Results and Discussion

The Pt L₃-edge XANES analysis of size-selected 0.8 ± 0.2 nm Pt NPs with 2D shape^[14] were measured as a function of H₂ pressure. In Figure 1 the normalized absorption coefficient of Pt NPs acquired in H₂ pressures of 1–21 bar and in 1 bar He, re-

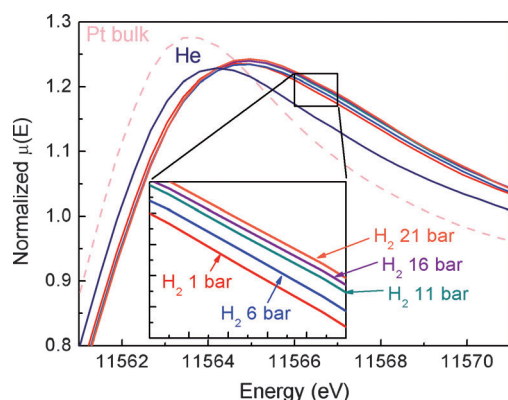


Figure 1. Pressure-dependent normalized absorption coefficient, $\mu(E)$, versus energy (XANES region) for the Pt L₃-edge of Pt NPs on γ -Al₂O₃. Data were acquired at pressures from 1 to 21 bar at 25 °C. Data acquired in He at 25 °C and Pt foil data are also plotted for reference.

spectively, at 25 °C is shown (1 bar = 100 kPa). A positive shift (+0.6 eV) in the absorption edge energy was observed upon hydrogen chemisorption as compared to the foil. Additionally, the intensity of the absorption peak (“white line”) was found to increase with increasing H₂ pressure, with adsorbate-free NPs measured in He showing a significantly lower intensity. The white-line intensity corresponds to the unoccupied 5d electron density of states, and its increase upon hydrogen adsorption reflects the transfer of charge from Pt to H. Furthermore, a broadening of the “white line” is observed upon hydrogen chemisorption. As shown in Refs. [6a, 13b,d, 15], the integrated area of the absorption peak can be used to extract quantitative information on the hydrogen coverage on the NPs. However, to conduct such analysis, a reference of the hydrogen-free state of the NPs is required. For this purpose, XANES data obtained in helium were used as a reference. To ensure that the Pt NPs were hydrogen-free during the measurements in helium after the NP reduction pretreatment in hydrogen, the reaction cell was pressurized to 4 bar He and heated to 375 °C for 30 min, then cooled to 25 °C in He before the measurements. An alternative approach (not used herein) to define the adsorbate-free state of the NPs involves the use of reference XANES data acquired under hydrogen at a high enough temperature at which negligible amounts of hydrogen would be adsorbed on the NP surface (375 °C for our Pt₂₂ NPs, as shown in Figure S2 in the Supporting Information), but this

approach may have added complexity due to the embedded effect of temperature.

To quantify the change in the hydrogen coverage on the NP surface under elevated H₂ pressure at 25 °C, Δ XANES plots were calculated. In Figure 2(a) the Δ XANES spectra for Pt NPs are shown, measured in 1–21 bar H₂ at 25 °C. An increase in

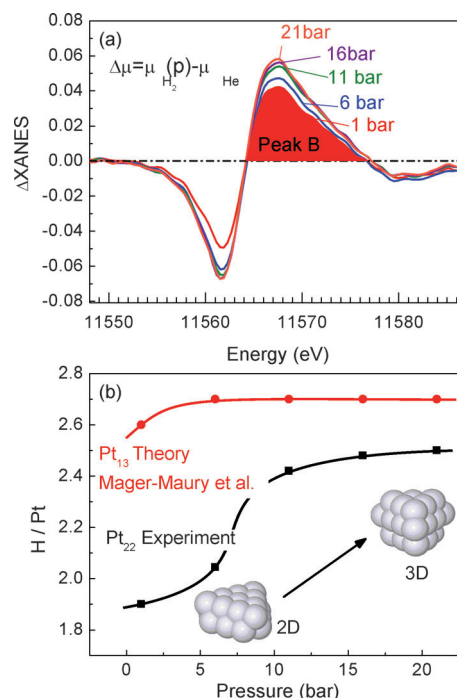


Figure 2. a) Δ XANES spectra from the Pt L₃-absorption edge of Pt NPs on γ -Al₂O₃ displayed as a function of the H₂ pressure during measurement. In all plots, the RT He data are subtracted from those acquired at varying pressures in H₂. b) H/Pt ratio calculated from the area of the Δ XANES peak B normalized by the area of bulk-like NPs measured at 183 K (■). Model shapes for low and high coverage are shown as well as theoretical H/Pt ratios from Ref. [6c] for Pt₁₃ NPs (●).

the area of peak B is seen with an increase in H₂ pressure, corresponding to an increase in H coverage on the NP surface. To estimate H/Pt ratios, the area of the Δ XANES peak B was normalized by the peak B area of large 1 nm diameter particles (Pt₁₄₀) with well-defined shape previously measured^[6a] in 1 bar H₂ at 183 K. Under these conditions, the larger NPs (Pt₁₄₀) are postulated to be saturated with one hydrogen atom per surface platinum atom. The number of hydrogen atoms per total number of Pt atoms in the Pt₂₂ NP are shown in Figure 2(b). To best compare our H/Pt ratios with those found in the literature, we normalized the hydrogen coverage by the total number of atoms in the NP, and not the number of Pt atoms at the surface, as was given in our previous work.^[6a] The hydrogen coverage on the NPs at 25 °C was found to increase from 1.9 to 2.5 H/Pt with an increase of pressure from 1 to 21 bar. Theoretical density functional theory (DFT) H/Pt ratios for Pt₁₃ NPs calculated by Mager-Maury et al.^[6c] are also plotted in Figure 2(b). For these smaller NPs, a higher H/Pt ratio of approximately 2.6 is seen at atmospheric pressure of H₂, which in-

creases only slightly with increasing H₂ pressure. This indicates that the smaller theoretical Pt₁₃ NPs are able to adsorb more hydrogen than our experimental Pt₂₂ NPs under equivalent conditions. This trend is in agreement with our previous work on Pt/γ-Al₂O₃ NPs showing that hydrogen adsorption capacity increases with decreasing particle size.^[6a] Similarly, Jensen et al.^[12b] obtained a saturation coverage of 2.9 H/Pt at 25 °C for their smaller Pt₁₃ NPs supported on a zeolite using H adsorption isotherms.

To investigate any morphological changes in the Pt NPs with increasing hydrogen coverage, EXAFS analysis was performed to extract 1st nearest-neighbor (NN) coordination number and bond length (*R*) information as a function of the hydrogen pressure. All EXAFS data from the reduced Pt NPs were fitted with two components corresponding to Pt–Pt (2.76 Å) and a long Pt–O (≈2.5 Å) bond.^[4d,15] The Pt–O component exhibits a longer bond length than that of the Pt oxide species or chemisorbed oxygen on Pt (≈2.0 Å), and is assigned to the NP/support interface.^[4d,15] The magnitude of the Fourier transform EXAFS data acquired in hydrogen at 25 °C from 1 bar to 21 bar is shown in Figures 3 together with an example fit as inset. The remainder of the 1st NN fits are shown in Figures S3–S7. In Table 1 EXAFS results are given for the Pt–Pt and Pt–O first-shell fits. In Figure 4, the Pt–Pt 1st NN coordination num-

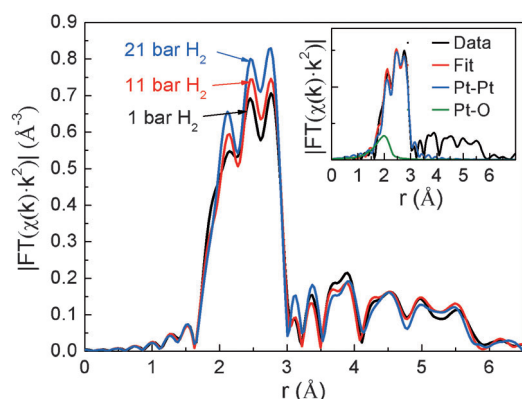


Figure 3. Fourier transform magnitudes of *k*²-weighted EXAFS data for Pt/γ-Al₂O₃ NPs measured at 25 °C under 1–21 bar H₂ pressure. A first shell fit of the experimental data measured under 11 bar H₂ is included as an inset.

H ₂ pressure [bar]	1 st NN (Pt–Pt)	<i>R</i> [Å] (Pt–Pt)	1 st NN (Pt–O)	<i>R</i> [Å] (Pt–O)
0 (He)	6.0 (7)	2.733 (5)	2 (1)	2.52 (3)
1	7.5 (7)	2.755 (4)	1.6 (8)	2.50 (4)
6	7.6 (7)	2.755 (4)	1.7 (9)	2.55 (4)
11	8.0 (7)	2.761 (4)	1.5 (8)	2.49 (5)
16	8.0 (7)	2.761 (3)	1.5 (8)	2.49 (4)
21	8.8 (8)	2.752 (3)	0.8 (7)	2.53 (8)

[a] The EXAFS fitting was performed with *S*₀² fixed at 0.85. The shared fit parameters Δ*E*₀ and σ² were Δ*E*₀ = 2.6 (5) eV and σ² = 0.0072 (4) Å².

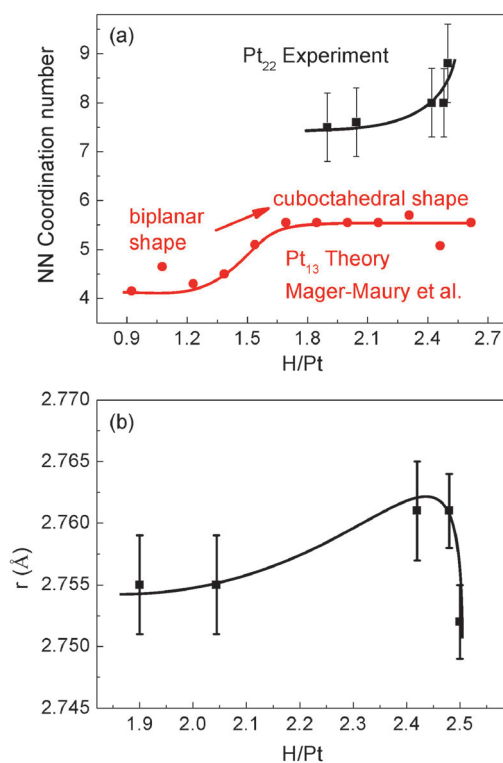


Figure 4. a) Pt–Pt 1st NN coordination number from EXAFS single-scattering analysis as a function of H coverage (■), and theoretical 1st NN coordination numbers for Pt₁₃ clusters from Ref. [6c] (●). b) Pt–Pt bond length (*r*) as a function of H coverage.

bers and Pt–Pt bond lengths are displayed for our Pt NPs under increasing H₂ pressure extracted from the analysis of EXAFS data, including NN data for Pt₁₃ clusters from Mager-Maury et al.^[6c] as a function of the H/Pt ratio.

Our results reveal that an increase in H₂ pressure correlates to an increase in Pt–Pt 1st NN from 7.5 to 8.8, which indicates a structural change in the NPs as the coverage of H increases. A significant change in Pt–Pt coordination number occurs between 16 and 21 bar, indicating a possible abrupt structural change at this pressure. The Pt–Pt 1st NN distance exhibits a slight increase with H₂ pressure up to 21 bar, at which point it drops. The Pt–O 1st coordination number decreases with increasing hydrogen pressure, indicating that Pt–O bonds between the metal and the hydroxylated Al₂O₃ support are broken. The increase in Pt–Pt coordination number and bond length, together with a concomitant decrease in the Pt–O coordination number, suggest that the NPs are restructured from their original 2D bilayer shape, modeled by our shape analysis,^[6a,14] to a more 3D-like structure upon hydrogen adsorption.

Previous theoretical studies have predicted hydrogen-induced morphological changes in subnanometer Pt NPs. For example, calculations by Mager-Maury et al.^[6c] on Pt₁₃ clusters supported on γ-Al₂O₃ revealed that they are stabilized in a 2D bilinear configuration at low hydrogen coverage caused by strong metal–support interactions. However, at coverages above approximately 1.5 H/Pt, these NPs are transformed to a 3D cuboctahedral shape as a result of a weakening of the

metal–support interaction by the adsorbed H, which is believed to accumulate at the NP/support interface and to contribute to NP/support bond breaking. A transformation from 2D to 3D shape would explain the increasing Pt–Pt coordination number with increasing H₂ pressure seen in this study, and also the drop in Pt–O coordination number as bonds between metal and support are broken. It should be, however, noted in Figure 4(a) that the calculations in Ref. [6c] revealed an approximately constant cuboctahedral shape for the high H/Pt coverages used in our study, because their Pt₁₃ NPs have already undergone a shape transformation from biplanar to cuboctahedral shape. It is plausible that their smaller Pt₁₃ NPs are more susceptible to shape transformation at lower H coverages because of their smaller size. Sintering could be another possible explanation for the increase in the Pt–Pt coordination number. Room-temperature Ostwald ripening has been reported for Pd nanoclusters upon exposure to hydrogen, which was explained by the formation of Pd hydride.^[17] Subsurface absorption of hydrogen would result in a decrease in Pt–Pt coordination numbers, which was not observed in this study. Therefore, room-temperature NP growth is not likely to occur in our samples, because they were also already preannealed in H₂ at much higher temperature (375 °C) without any evidence of sintering.^[14b] Although our results show no evidence for subsurface hydrogen, surface hydride species may still form on our NPs. However, Pt NPs are not known to form hydrides, but Hakamada et al.^[18] reported that nanoporous Pt could form hydride species under lattice strain.^[18] In addition, theoretical studies predict the formation of Pt hydrides on nanoparticles at high H coverage.^[6c, 11b]

Recent work by Jensen et al.^[12b] has provided experimental evidence for Pt NPs restructuring under hydrogen pressure. Their Pt₁₃/KL zeolite NPs were measured by EXAFS after reduction in H₂ and after H desorption by heating at 573 K. Upon desorbing H, the Pt–Pt coordination number decreases, Pt–O coordination number increases, and the Pt–Pt bond length decreases, which the authors attribute to a restructuring of the NP to a flatter shape with more support interaction. DFT calculations by Chen et al.^[11b] also predicted restructuring for unsupported Pt₁₃ NPs, which undergo a phase transformation from icosahedral to face-centered cubic structure at approximately 0.8 H/Pt, and above 2.8 H/Pt, H atoms can penetrate into the structure.

In our study, the Pt–Pt bond length shown in Figure 4(b) increases with increasing hydrogen pressure until a coverage of 2.5 H/Pt is reached, at which point the bond length drops. For nanometer-sized Pt NPs, the Pt–Pt bond length has been shown to increase with increasing hydrogen coverage caused by a lifting of the bond-length contraction by the adsorbed hydrogen.^[8c, 10c, 12a, 19] A structural change in the NPs to a more 3D shape with a lower fraction of atoms at the surface would also relieve surface strain responsible for bond contraction. The anomalous drop in bond length measured at the highest pressure does not fit the previously described trends, but might be plausible if the strain induced by the NP support is initially expansive, in which case the NP break off from the support would result in Pt–Pt bond length contraction. Indeed, DFT cal-

culations by Hu et al.^[10a] predict that for the majority of stable Pt₁₃ cluster shapes, the γ -Al₂O₃ support induces an expansion in the Pt–Pt distance compared to that of unsupported NPs. Alternatively, this drop could be related to decomposition of surface hydride species at high hydrogen pressures, which was seen on nanoporous Pt above 13 bar H₂ pressure.^[18] Nevertheless, it should be noted that as no loss of hydrogen was observed at this pressure through XANES analysis, the latter possibility is unlikely.

The present work illustrates the intricate correlation between the NP environment (surrounding adsorbates and support) and the electronic and structural characteristics of small NPs. To gain further insight into these effects, additional studies are planned with Pt NPs of different size and shape, and to extend the H₂ pressure regime to higher values.

Conclusions

An in situ investigation of the role of chemisorbed hydrogen on the electronic and structural properties of size-controlled Pt nanoparticles (NPs) supported on γ -Al₂O₃ was performed by means of X-ray absorption near-edge structure (XANES) and extended X-ray-absorption fine-structure (EXAFS) measurements. In situ XANES measurements on approximately 0.8 nm Pt NPs (Pt₂₂) revealed an increase in the hydrogen coverage on the surface of the NPs (H/Pt ratio) with increasing hydrogen pressure from 1 to 21 bar at 25 °C. Furthermore, EXAFS measurements revealed a change in the structure of the NPs from 2D to 3D, evidenced by increasing Pt–Pt coordination numbers and decreasing Pt–O (NP/support interface) coordination numbers. This study highlights the dynamic nature of NP catalysts under industrially relevant conditions and the superior adsorption capacity of subnanometer particles, properties that have high importance to catalyst design.

Experimental Section

Pt/ γ -Al₂O₃ NPs were prepared in solution through inverse micelle encapsulation. A PS-*b*-P2VP diblock copolymer was dissolved in toluene to create micellar cages, which were then loaded with Pt by adding H₂PtCl₆ to the solution and stirring for 2 days. The molar ratio of Pt to polymer P2VP was 0.05. The solution was then filtered, nanocrystalline γ -Al₂O₃ powder (average grain size 40 nm) was added, and then the solution was stir-dried in air at 60 °C. The Pt/ γ -Al₂O₃ NPs were then calcined at 375 °C in O₂ for 24 h to remove the polymer, and X-ray photoelectron spectroscopy was used to demonstrate that the encapsulating polymers were completely removed, as indicated by the absence of a C 1s signal. The size and shape of the prepared NPs was determined using a combination of low-temperature EXAFS multiple scattering analysis and TEM diameter measurements. Details on the shape analysis are given in Figure S1. The above synthesis resulted in size-selected Pt NPs (0.8 ± 0.2 nm), with approximately 22 atoms (Pt₂₂) in a flat (2D) bilayer shape.^[14]

XAFS measurements were performed at Beamline 10-ID-B of the Advanced Photon Source at Argonne National Laboratory. The Pt/ γ -Al₂O₃ sample (60 mg) was loaded into an in situ beryllium high-pressure reaction cell allowing pressurization above 20 bar.^[20] The

reaction cell was housed within a furnace allowing for sample heating by means of an external PID temperature controller. The Pt L₃-edge was measured in transmission mode, and at least three spectra were acquired at each pressure condition for signal averaging. The gas flows were controlled using Brooks mass flow controllers. The sample was first reduced in 50% H₂ balanced by He at a flow of 50 mL min⁻¹ at 375 °C. Next, the sample was cooled to 25 °C and measured at atmospheric pressure in H₂, then measurements were taken after the cell was pressurized to 6, 11, 16, and 21 bar of H₂. The reactor was then depressurized to 4 bar, flushed with He, and heated to 375 °C to remove all H₂ from the sample, and a measurement of the adsorbate-free NPs was taken at 25 °C in 4 bar He. A final set of measurements was taken at 375 °C in H₂ pressures of 0.15, 0.5, and 3 bar.

Data processing was conducted using the IFEFFIT^[21] package. By using the Athena software,^[22] reference spectra from each measurement were aligned to a Pt reference foil, and then data were merged and normalized by fitting smooth curves to the pre-edge and post-edge. Δ XANES plots were constructed by subtracting the spectra measured in He at 25 °C from spectra measured at various pressures of H₂. Owing to the presence of isosbestic points in XANES data at different hydrogen coverages, the Δ XANES data crosses the zero value at the same energies for all different H coverages. The area of the second Δ XANES peak, "peak B"^[6a] (marked in Figure 2a), was integrated by using OriginLab software over the energy range in which peak B was positive. EXAFS spectra were fit in R-space in the Artemis software^[22] with FEFF8 calculations of face-centered cubic Pt to simulate Pt–Pt scattering paths and the Pt–O scattering path from Na₂Pt(OH)₆ to simulate Pt–O scattering paths. Data sets measured under different pressures were fit simultaneously with the energy shift ΔE_0 constrained, and owing to the strong correlation between Pt–Pt coordination number and bond length disorder (σ^2), σ^2 was fit as a shared parameter. Additional fit details and example fits are given in the Supporting Information.

Acknowledgements

The support of Prof. Carlo Segre from the Illinois Institute of Technology setting up the XAFS beamline at ANL is greatly appreciated. In addition, the authors are grateful to Lindsay R. Merte, Estephania Lira, and Sudeep Pandey for their assistance with the EXAFS measurements. Use of the Advanced Photon Source was supported by the U.S. Department of Energy, Office of science, Office of basic Energy Sciences, under contract No. DE-AC02-06CH11357. MRCAT operations are supported by the Department of Energy and the MRCAT member institutions. This work was funded by the Office of Basic Energy Sciences from the US Department of Energy under contract DE-FG02-08ER15995.

Keywords: hydrogen · nanoparticles · platinum · structure elucidation · X-ray absorption spectroscopy

- [1] a) F. Zaera, *Phys. Chem. Chem. Phys.* **2013**, 11988–12003; b) P. Rylander, *Catalytic Hydrogenation over Platinum Metals*, Academic Press, **1967**.
[2] a) C. Cui, M. Ahmadi, F. Behafarid, L. Gan, M. Neumann, M. Heggen, B. Roldan Cuenya, P. Strasser, *Faraday Discuss.* **2013**, 162, 91–112; b) A. Wieckowski, E. R. Savinova, C. G. Vayenas, *Catalysis and Electrocatalysis at Nanoparticle Surfaces*, CRC Press, **2003**.
[3] a) Y. Li, R. T. Yang, *J. Phys. Chem. C* **2007**, 111, 11086–11094; b) L. Wang, R. T. Yang, *J. Phys. Chem. C* **2008**, 112, 12486–12494.

- [4] a) S. Mukerjee, *J. Appl. Electrochem.* **1990**, 20, 537–548; b) M. Yamauchi, H. Kobayashi, H. Kitagawa, *ChemPhysChem* **2009**, 10, 2566–2576; c) B. Roldan Cuenya, *Thin Solid Films* **2010**, 518, 3127–3150; d) M. Vaarkamp, J. T. Miller, F. S. Modica, D. C. Koningsberger, *J. Catal.* **1996**, 163, 294–305.
[5] C. Zhou, J. Wu, A. Nie, R. C. Forrey, A. Tachibana, H. Cheng, *J. Phys. Chem. C* **2007**, 111, 12773–12778.
[6] a) F. Behafarid, L. Ono, S. Mostafa, J. Croy, G. Shafai, S. Hong, T. Rahman, S. R. Bare, B. Roldan Cuenya, *Phys. Chem. Chem. Phys.* **2012**, 14, 11766–11779; b) M. K. Oudenhuijzen, J. A. van Bokhoven, J. T. Miller, D. E. Ramaker, D. C. Koningsberger, *J. Am. Chem. Soc.* **2005**, 127, 1530–1540; c) C. Mager-Maury, G. Bonnard, C. Chizallet, P. Sautet, P. Raybaud, *ChemCatChem* **2011**, 3, 200–207.
[7] L. Spenadel, M. Boudart, *J. Phys. Chem.* **1960**, 64, 204–207.
[8] a) B. Kip, F. Duivenvoorden, D. Koningsberger, R. Prins, *J. Catal.* **1987**, 105, 26–38; b) J. Singh, R. C. Nelson, B. C. Vicente, S. L. Scott, J. A. van Bokhoven, *Phys. Chem. Chem. Phys.* **2010**, 12, 5668–5677; c) E. Bus, J. A. van Bokhoven, *Phys. Chem. Chem. Phys.* **2007**, 9, 2894–2902.
[9] a) P. S. Petkov, G. P. Petrova, G. N. Vayssilov, N. Röscher, *J. Phys. Chem. C* **2010**, 114, 8500–8506; b) A. Vargas, G. Santarossa, A. Baiker, *J. Phys. Chem. C* **2011**, 115, 10661–10667; c) X. Liu, H. Dilger, R. Eichel, J. Kunstmann, E. Roduner, *J. Phys. Chem. B* **2006**, 110, 2013–2023.
[10] a) C. H. Hu, C. Chizallet, C. Mager-Maury, M. Corral-Valero, P. Sautet, H. Toulhoat, P. Raybaud, *J. Catal.* **2010**, 274, 99–110; b) Y. Lei, J. Jelic, L. C. Nitsche, R. Meyer, J. Miller, *Top. Catal.* **2011**, 54, 334–348; c) S. I. Sanchez, L. D. Menard, A. Bram, J. H. Kang, M. W. Small, R. G. Nuzzo, A. I. Frenkel, *J. Am. Chem. Soc.* **2009**, 131, 7040–7054.
[11] a) G. Rupprechter, H.-J. Freund, *Top. Catal.* **2000**, 14, 3–14; b) L. Chen, C.-g. Zhou, J.-p. Wu, H.-s. Cheng, *Front. Phys. China* **2009**, 4, 356–366.
[12] a) M. W. Small, S. I. Sanchez, N. S. Marinkovic, A. I. Frenkel, R. G. Nuzzo, *ACS Nano* **2012**, 6, 5583–5595; b) C. Jensen, D. Buck, H. Dilger, M. Bauer, F. Phillipp, E. Roduner, *Chem. Commun.* **2013**, 49, 588–590.
[13] a) Y. Ji, V. Koot, A. M. van der Eerden, B. M. Weckhuysen, D. C. Koningsberger, D. E. Ramaker, *J. Catal.* **2007**, 245, 415–427; b) N. Guo, B. R. Fingland, W. D. Williams, V. F. Kispersky, J. Jelic, W. N. Delgass, F. H. Ribeiro, R. J. Meyer, J. T. Miller, *Phys. Chem. Chem. Phys.* **2010**, 12, 5678–5693; c) O. S. Alexeev, F. Li, M. D. Amiridis, B. C. Gates, *J. Phys. Chem. B* **2005**, 109, 2338–2349; d) T. Kubota, K. Asakura, N. Ichikuni, Y. Iwasawa, *Chem. Phys. Lett.* **1996**, 256, 445–448; e) D. Ramaker, D. Koningsberger, *Phys. Chem. Chem. Phys.* **2010**, 12, 5514–5534; f) S. N. Reifsnnyder, M. M. Otten, D. E. Sayers, H. H. Lamb, *J. Phys. Chem. B* **1997**, 101, 4972–4977; g) S. Bordiga, E. Groppo, G. Agostini, J. A. van Bokhoven, C. Lamberti, *Chem. Rev.* **2013**, 113, 1736–1850; h) M. Teliska, W. O'Grady, D. Ramaker, *J. Phys. Chem. B* **2004**, 108, 2333–2344.
[14] a) B. Roldan Cuenya, M. A. Ortigoza, L. Ono, F. Behafarid, S. Mostafa, J. Croy, K. Paredis, G. Shafai, T. Rahman, L. Li, *Phys. Rev. B* **2011**, 84, 245438; b) B. Roldan Cuenya, J. R. Croy, S. Mostafa, F. Behafarid, L. Li, Z. Zhang, J. C. Yang, Q. Wang, A. I. Frenkel, *J. Am. Chem. Soc.* **2010**, 132, 8747–8756.
[15] A. Y. Stakheev, Y. Zhang, A. Ivanov, G. Baeva, D. Ramaker, D. Koningsberger, *J. Phys. Chem. C* **2007**, 111, 3938–3948.
[16] a) K. Paredis, L. K. Ono, F. Behafarid, Z. Zhang, J. C. Yang, A. I. Frenkel, B. Roldan Cuenya, *J. Am. Chem. Soc.* **2011**, 133, 13455–13464; b) Y. Zhang, M. L. Toebe, A. van der Eerden, W. E. O'Grady, K. P. de Jong, D. C. Koningsberger, *J. Phys. Chem. B* **2004**, 108, 18509–18519; c) L. R. Merte, M. Ahmadi, F. Behafarid, L. K. Ono, E. Lira, J. Matos, L. Li, J. C. Yang, B. Roldan Cuenya, *ACS Catal.* **2013**, 130517100016006.
[17] M. Di Vece, D. Grandjean, M. Van Bael, C. Romero, X. Wang, S. Decoster, A. Vantomme, P. Lievens, *Phys. Rev. Lett.* **2008**, 100, 236105.
[18] M. Hakamada, T. Furukawa, T. Yamamoto, M. Takahashi, M. Mabuchi, *Mater. Trans.* **2011**, 52, 806–809.
[19] E. Bus, J. T. Miller, A. J. Kropf, R. Prins, J. A. van Bokhoven, *Phys. Chem. Chem. Phys.* **2006**, 8, 3248–3258.
[20] S. R. Bare, N. Yang, S. D. Kelly, G. E. Mickelson, F. S. Modica, *Catal. Today* **2007**, 126, 18–26.
[21] M. Newville, *J. Synchrotron Radiat.* **2001**, 8, 322–324.
[22] B. Ravel, M. Newville, *J. Synchrotron Radiat.* **2005**, 12, 537–541.

Received: September 17, 2013

Published online on November 15, 2013